A&A 418, 363–369 (2004)
DOI: 10.1051/0004-6361:20034384

Astronomy & Astrophysics

Electron impact excitation of fine-structure levels in Cl II⋆

S. S. Tayal⋆⋆

Department of Physics, Clark Atlanta University, Atlanta, GA 30314, USA

Received 23 September 2003 / Accepted 7 November 2003

Abstract. The B-spline basis has been used in the R-matrix approach to calculate electron impact excitation collision strengths for transitions between the $3s^23p^4\ ^3P_{0,1,2}$, $^1D_2$ and $^1S_0$ levels and from these levels to the fine-structure levels of the excited $3s3p^5$, $3s^23p^34s$, $3s^23p^33d$, $3s^23p^34p$ and $3s^23p^34d$ configurations of Cl II. We considered 23 LS states $3s^23p^4\ ^3P$, ^1D, ^1S, $3s3p^5\ ^3P^\circ$, $3s^23p^3(^4S^\circ)4s\ ^{5,3}S^\circ$, $3s^23p^3(^4S^\circ)3d\ ^{5,3}D^\circ$, $3s^23p^3(^2D^\circ)3d\ ^1P^\circ$, $^1S^\circ$, $^3F^\circ$, $^3D^\circ$, $^3P^\circ$, $3s^23p^3(^2D^\circ)4s\ ^{3,1}D^\circ$, $3s^23p^3(^2P^\circ)4s\ ^{3,1}P^\circ$, $3s^23p^3(^4S^\circ)4p\ ^{5,3}P$, $3s^23p^3(^2P^\circ)3d\ ^{3,1}P^\circ$, $^3D^\circ$ and $3s^23p^3(^2D^\circ)4d\ ^3P^\circ$ in the close-coupling expansion that give rise to 51 fine-structure levels. The non-orthogonal orbitals are used for an accurate representation of both the target wavefunctions and the R-matrix basis functions. The collision strengths for transitions between fine-structure levels are calculated by transforming the LS-coupled K-matrices to K-matrices in an intermediate coupling scheme. The Rydberg series of resonances converging to excited state thresholds make substantial contributions to collision strengths. The thermally averaged collision strengths have been obtained by integrating collision strengths over a Maxwellian distribution of electron energies and these are listed in Table 2 for log T from 3.3 to 5.6 K.

Key words. atomic data – atomic processes – line: formation

1. Introduction

The fine-structure transitions among the levels of ground $3s^23p^4$ configuration in Cl II give rise to spectral lines in the infrared and visible part of the spectrum and transitions from the ground configuration to excited $3s3p^5$, $3s^23p^34s$, $3s^23p^33d$, $3s^23p^34p$ and $3s^23p^34d$ configurations occur in the ultraviolet (UV), far-ultraviolet (FUV) and extreme ultraviolet (EUV) wavelength regions. Emission lines of collisionally excited Cl II have been detected in the spectra of the Io torus from the ground-based observations (Küppers & Schneider 2000) as well as from the space-based observations by the Far-Ultraviolet Spectroscopic Explorer (FUSE) (Feldman et al. 2001). Electron-ion collision processes play an important role in the understanding of energy balance in various types of plasmas. Accurate electron impact collision strengths of fine-structure transitions in Cl II are needed for the interpretation of observed spectra to understand the physical processes and conditions such as temperature, density and chlorine abundance in Io-torus-Jupiter system.

The strong mixing between a number of levels of the different Rydberg $3s^23p^3nl$ series and the $3s3p^5$ perturber states are caused by configuration-interaction (Tayal 2003). The Cl II wavefunctions show strong term dependence of the one-electron orbitals and large correlation corrections. The term dependent non-orthogonal orbitals in the multiconfiguration Hartree-Fock approach (Froese Fischer 1991; Zatsarinny & Froese Fischer 1999) have been used to provide adequate treatment of large correlation corrections as well as the interactions between different Rydberg series and perturber states. These wavefunctions yield excitation energies of Cl II target states that are in excellent agreement with the experimental values. The B-spline R-matrix approach (Zatsarinny & Froese Fischer 1999; Zatsarinny & Tayal 2001) has been used to calculate electron impact excitation collision strengths and effective collision strengths for all dipole allowed, intercombination and forbidden transitions among the fine-structure levels. Our calculation included 23 spectroscopic bound states of Cl II in the close-coupling expansion. We included 15 states $3s^23p^4\ ^3P$, ^1D, ^1S, $3s3p^5\ ^3P^\circ$, $3s^23p^3(^4S^\circ)4s\ ^{5,3}S^\circ$, $3s^23p^3(^4S^\circ)3d\ ^{5,3}D^\circ$, $3s^23p^3(^2D^\circ)3d\ ^1P^\circ$, $^1S^\circ$, $^3F^\circ$, $3s^23p^3(^2D^\circ)4s\ ^{3,1}D^\circ$, $3s^23p^3(^4S^\circ)4p\ ^{5,3}P$ and eight higher-lying states $3s^23p^3(^2P^\circ)4s\ ^{3,1}P^\circ$, $3s^23p^3(^2P^\circ)3d\ ^3D^\circ$, $^3P^\circ$, $^1P^\circ$, $3s^23p^3(^2D^\circ)3d\ ^3D^\circ$, $^3P^\circ$, $3s^23p^3(^2D^\circ)4d\ ^1P^\circ$ which have strong dipole connection with the $3s^23p^4$ terms. A B-spline basis has been used for the description of continuum functions. No orthogonality constraint has been imposed on the continuum functions and atomic bound orbitals. This procedure leads to substantial reduction in pseudo-resonances in the electron collisional excitation strengths. The completeness of the B-spline ensures that no Buttle correction to the R-matrix elements is required.

Recently, Wilson & Bell (2002) reported collision data for the 10 fine-structure transitions among the ground configuration levels $3s^23p^4\ ^3P_{0,1,2}$, $^1D_2$ and $^1S_0$ of Cl II. They included lowest 12 LS states $3s^23p^4\ ^3P$, ^1D, ^1S, $3s3p^5\ ^3P^\circ$,

⋆ Table 2 is only available in electronic form at CDS via anonymous ftp to cdsarc.u-strasbg.fr (130.79.128.5) or via http://cdsweb.u-strasbg.fr/cgi-bin/qcat?J/A+A/418/363

⋆⋆ e-mail: stayal@cau.edu

$3s^23p^3(^4S^\circ)4s\ ^{5,3}S^\circ$, $3s^23p^3(^4S^\circ)3d\ ^{5,3}D^\circ$, $3s^23p^3(^2D^\circ)3d\ ^1P^\circ$, $^1S^\circ$, $^3F^\circ$ and $3s^23p^3(^2D^\circ)4s\ ^3D^\circ$ in the close-coupling expansion in their R-matrix calculations and used configuration-interaction (CI) wavefunctions (Hibbert 1975) for these target states that were constructed with eight spectroscopic 1s, 2s, 2p, 3s, 3p, 3d, 4s and 4p orbitals and two pseudo-orbitals 4d and 4f. Earlier, a theoretical calculation of electron impact excitation of Cl II was reported by Krueger & Czyzak (1970) using a distorted wave approximation and using Hartree-Fock (HF) representation of Cl II target states. Berrington & Nakazaki (2002) reported bound state energies, oscillator strengths and ground state photoionization cross sections for chlorine and its ions. Tayal (2003) investigated the term dependence of wavefunctions, interactions between the different $^3P^\circ$, $^1P^\circ$ and $^3D^\circ$ Rydberg series and importance of correlation corrections in Cl II using the non-orthogonal orbitals.

2. Details of collision calculation

Accurate representation of target wavefunctions is an essential ingredient of a reliable collision calculation. The target states in our calculation are accurately represented by non-orthogonal orbitals obtained by separate optimization of each target state. The non-orthogonal orbitals allow to include correlation corrections with a minimum number of configurations and correlated orbitals. However, non-orthogonal orbitals technique is computationally more time consuming than the orthogonal orbitals. Earlier calculation of Cl II wavefunctions by Wilson & Bell (2002) used the same set of orthogonal orbitals. They included a pseudo-orbital 4d to account for the term dependence of 3d orbital and a pseudo-orbital 4f to include correlation corrections. In our calculation we used non-orthogonal orbitals for the description of term-dependence of radial functions. The 3s and 3p orbitals in the $3s^23p^4$ and $3s3p^5$ configurations are similar, but differ in the $3s^23p^4$ and $3s^23p^3nl$ configurations. We used two different sets of 3s and 3p orbitals; one for the $3s^23p^4$ and $3s3p^5$ configurations and another for the $3s^23p^3nl$ configurations. Different valence 4s, 4p, 3d and 4d orbitals are obtained for the individual $3s^23p^3(^4S^\circ,\ ^2D^\circ,\ ^2P^\circ)nl\ ^{1,3,5}L$ ($L = 0, 1, 2, 3$) states in separate calculations. Additional to spectroscopic orbitals we obtained several s, p, d and f correlation orbitals to account for core correlation, core-polarization or core-valence correlation and interactions between different Rydberg series. The mean radii of the correlation orbitals are comparable to the 3s, 3p, 3d, 4s and 4p spectroscopic orbitals and thus represent the correlation corrections very well. We found that the core-valence correlation where one electron from the 3s subshell of the $3s^23p^3$ core is excited to the outer orbitals and core correlation $3s^23p^3 \rightarrow 3p^5$ represent large correlation corrections.

The wave function describing the total $(N+1)$-electron system in the internal region surrounding the atom with radius $r \le a$ is expanded in terms of energy-independent functions (Berrington et al. 1995)

$$\Psi_k = A \sum_{ij} a_{ijk} \overline{\Phi_i} u_j(r) + \sum_j b_{jk} \phi_j, \quad (1)$$

where $\overline{\Phi_i}$ are channel functions formed from the multi-configurational functions of the target states and u_j are the radial basis functions describing the motion of the scattering electron. The operator A antisymmetrizes the wave function and a_{ijk} and b_{jk} are expansion coefficients determined by diagonalizing the $(N+1)$-electron Hamiltonian. The functions ϕ_j in Eq. (1) are of bound-state type and are included to allow for short-range correlation effect. In our R-matrix calculation, the radial functions u_j are expanded in the spline basis as

$$u_j(r) = \sum_i \overline{a_{ij}} B_i(r), \quad (2)$$

and the coefficients $\overline{a_{ij}}$ (which now replace a_{ijk} in Eq. (1)) and coefficients b_{jk} are determined by diagonalizing the $(N+1)$-electron Hamiltonian inside the R-matrix box of radius a that contain all bound atomic orbitals used for the description of Cl II states. We used 96 continuum basis functions for each orbital angular momentum and a boundary radius $a = 25$ au. For an accurate determination of electron flux through the boundary, we do not impose any boundary condition on u_j functions at the outer edge of the box. The amplitudes of the wavefunctions at the boundary which are needed for construction of the R-matrix are simply given by the coefficient of the last spline. The completeness of the B-spline basis ensures that no Buttle correction to the R-matrix elements is required. The R-matrix calculations with inclusion of exchange were carried out for all partial waves with $L \le 20$.

The LS-coupled K-matrices are calculated by matching the inner region solutions at $r = a$ with asymptotic solutions in the outer region. The FARM program (Burke & Noble 1995) has been used to find the asymptotic solutions. The collision strengths between fine-structure levels are calculated by transforming the LS-coupled K-matrices to K-matrices in an intermediate coupling scheme. We have used the intermediate-coupling frame transformation (ICFT) method (Giffin et al. 1998). This method employs multi-channel quantum defect theory (MQDT) to generate unphysical K-matrices in LS coupling and these are transformed to intermediate coupling. The physical K-matrices are then obtained from the intermediate-coupled unphysical K-matrices. The higher partial wave contributions for the dipole-allowed and other transitions are calculated using a top-up procedure based on the geometric series approximation (Burgess et al. 1970).

In the asymptotic region, the collision strength follows a high energy limiting behavior which is determined by the type of transition. For optically allowed electric-dipole transitions

$$\Omega_{if}(E) \sim_{E\to\infty} d\ \ln(E), \quad (3)$$

where the parameter d is propotional to the oscillator strength. In the case of the multipole optically forbidden transitions such as electric quadrupole or magnetic dipole transitions

$$\Omega_{if}(E) \sim_{E\to\infty} constant, \quad (4)$$

where the value of *constant* can be obtained from the Bethe approximation. The intercombination transitions have the asymptotic form

$$\Omega_{if}(E) \sim_{E\to\infty} \frac{1}{E^2}. \quad (5)$$

The rapid decrease of collision strengths with incident electron energies in the case of intercombination transitions is due to the fact that these transitions can only occur through electron exchange.

In many applications it is convenient to use excitation rate coefficients or thermally averaged collision strengths as a function of electron temperature. The electron excitation rates are obtained by averaging total collision strengths over a Maxwellian distribution of electron energies. The excitation rate coefficient for a transition from state i to state f at electron temperature T_e is given by

$$C_{if} = \frac{8.629 \times 10^{-6}}{g_i T_e^{1/2}} \gamma_{if}(T_e) \exp\left(\frac{-\Delta E_{if}}{kT_e}\right) \text{ cm}^3 \text{ s}^{-1}, \quad (6)$$

where g_i is the statistical weight of the lower level i, $\Delta E_{if} = E_f - E_i$ is the excitation energy, and γ_{if} is a dimensionless quantity called effective collision strength and is given by

$$\gamma_{if}(T_e) = \int_0^\infty \Omega_{if} \exp\left(\frac{-E_f}{kT_e}\right) \mathrm{d}\left(\frac{E_f}{kT_e}\right), \quad (7)$$

where Ω_{if} is the total collision strength for transitions between levels i and f, k is the Boltzmann constant, and E_f is the energy of incident electron with respect to the upper level f. If the collision strength is assumed to be independent of the incident electron energy, we have $\gamma_{if} = \Omega_{if}$.

The effective collision strengths are calculated by integrating collision strengths for fine-structure levels over a Maxwellian distribution of electron energies.

3. Results and discussion

Our target wavefunctions correctly represent the main correlation corrections and the interaction between different Rydberg series and perturbers as indicated by excellent agreement between the calculated excitation energies and experimental values. Excitation energies of the 23 LS Cl II target states relative to the ground state are presented in Table 1 where our calculated results are compared with the experimental values from the National Institute of Standard and Technology (NIST) (`http://physics.nist.gov`) and the calculations of Wilson & Bell (2002) and Berrington & Nakazaki (2002). Wilson & Bell (2002) calculated wavefunctions for the 12 LS Cl II states and Berrington & Nakazaki (2002) used R-matrix method (Berrington et al. 1995) to obtain radiative data for a large number of Cl II terms. Our calculation shows very good agreement with the calculation of Berrington & Nakazaki (2002) except for the assignments of the lowest ^{1}P° and third lowest ^{1}P° states. In our calculation these ^{1}P° states belong to the $3s3p^5$ and $3s^23p^3(^2D°)4d$ configurations which agree with the NIST compilation. The labeling of these two states from the calculation of Berrington & Nakazaki (2002) has been changed in Table 1 to match our assignments. Our calculation is in better agreement with the measured values for most states than the calculation of Wilson & Bell (2002). The $3s3p^5$ ^{3}P° state in our calculation is slightly over correlated compared to the ground state.

Table 1. Excitation energies of Cl II states relative to the ground state. Present theory is compared with the NIST compilation (`http://physics.nist.gov`) and the calculations of Wilson & Bell (2002) (WB) and Berrington & Nakazaki (2002) (BN).

State	Present theory	Experiment	WB	BN
$3s^23p^4$ ^{3}P	0.0000	0.0000	0.0000	0.0000
$3s^23p^4$ ^{1}D	0.1058	0.1031	0.1103	0.1082
$3s^23p^4$ ^{1}S	0.2526	0.2509	0.2589	0.2675
$3s3p^5$ ^{3}P°	0.8210	0.8506	0.8301	0.8500
$3s^23p^3(^4S°)4s$ ^{5}S°	0.9813	0.9800	0.9788	0.9791
$3s^23p^3(^4S°)3d$ ^{5}D°	0.9962	1.0020	0.9949	1.0044
$3s^23p^3(^4S°)4s$ ^{3}S°	1.0242	1.0231	1.0352	1.0221
$3s^23p^3(^2D°)3d$ ^{1}P°	1.0353	1.0508	1.0457	1.0596[a]
$3s^23p^3(^4S°)3d$ ^{3}D°	1.0875	1.0887	1.1033	1.0973
$3s^23p^3(^2D°)3d$ ^{1}S°	1.1319	1.1382	1.1281	1.1481
$3s^23p^3(^2D°)3d$ ^{3}F°	1.1554	1.1476	1.1627	1.1617
$3s^23p^3(^2D°)4s$ ^{3}D°	1.1742	1.1520	1.1743	1.1677
$3s^23p^3(^4S°)4p$ ^{5}P	1.1721	1.1696		1.1634
$3s^23p^3(^2D°)4s$ ^{1}D°	1.1903	1.1730		1.1886
$3s^23p^3(^4S°)4p$ ^{3}P	1.2063	1.1976		1.1921
$3s^23p^3(^2P°)4s$ ^{3}P°	1.2726	1.2526		1.2752
$3s^23p^3(^2P°)4s$ ^{1}P°	1.2939	1.2750		1.2980
$3s^23p^3(^2D°)3d$ ^{3}D°	1.3203	1.2828		1.2959
$3s^23p^3(^2P°)3d$ ^{3}P°	1.3420	1.3248		1.3472
$3s^23p^3(^2P°)3d$ ^{3}D°	1.4482	1.3719		1.3881
$3s^23p^3(^2D°)3d$ ^{3}P°	1.4905	1.4310		1.4534
$3s^23p^3(^2D°)4d$ ^{1}P°	1.5343	1.4842		1.5013[a]
$3s^23p^3(^2P°)3d$ ^{1}P°	1.5984	1.5480		1.5718

[a] The labeling of these states from Berrington & Nakazaki (2002) are changed to match our assignments.

We chose a fine energy mesh (0.0002 Ryd) for collision strengths calculation in the thresholds energy region which allowed us to include resonance structures accurately. We calculated collision strengths at 8150 energy points in the thresholds region upto 1.60 Ryd and at 150 energy points in the above threshold region upto 16.6 Ryd. The collision strengths are displayed as a function of electron energy for the low-lying forbidden $3s^23p^4$ $^3P_1$–$3s^23p^4$ $^3P_2$, $3s^23p^4$ $^3P_1$–$3s^23p^4$ $^1D_2$ and $3s^23p^4$ $^1D_2$–$3s^23p^4$ $^1S_0$ transitions in Figs. 1–3 respectively in the thresholds energy region. Our results can be compared with 12-state R-matrix calculation of Wilson & Bell (2002) (not shown). Both calculations exhibit similar complicated resonance structure because of the interference and overlapping of several Rydberg series of resonances. Our calculation includes additional resonances converging to higher excited states above 1.15 Ryd because of the inclusion of additional 11 target states in the close-coupling expansion in our work that have thresholds between 1.172 Ryd and 1.598 Ryd. It is clear that these resonances converging to higher excited states make significant contributions. There seem to be some differences in the background collision strengths away from resonances from the two calculations. These differences can be clearly noted for

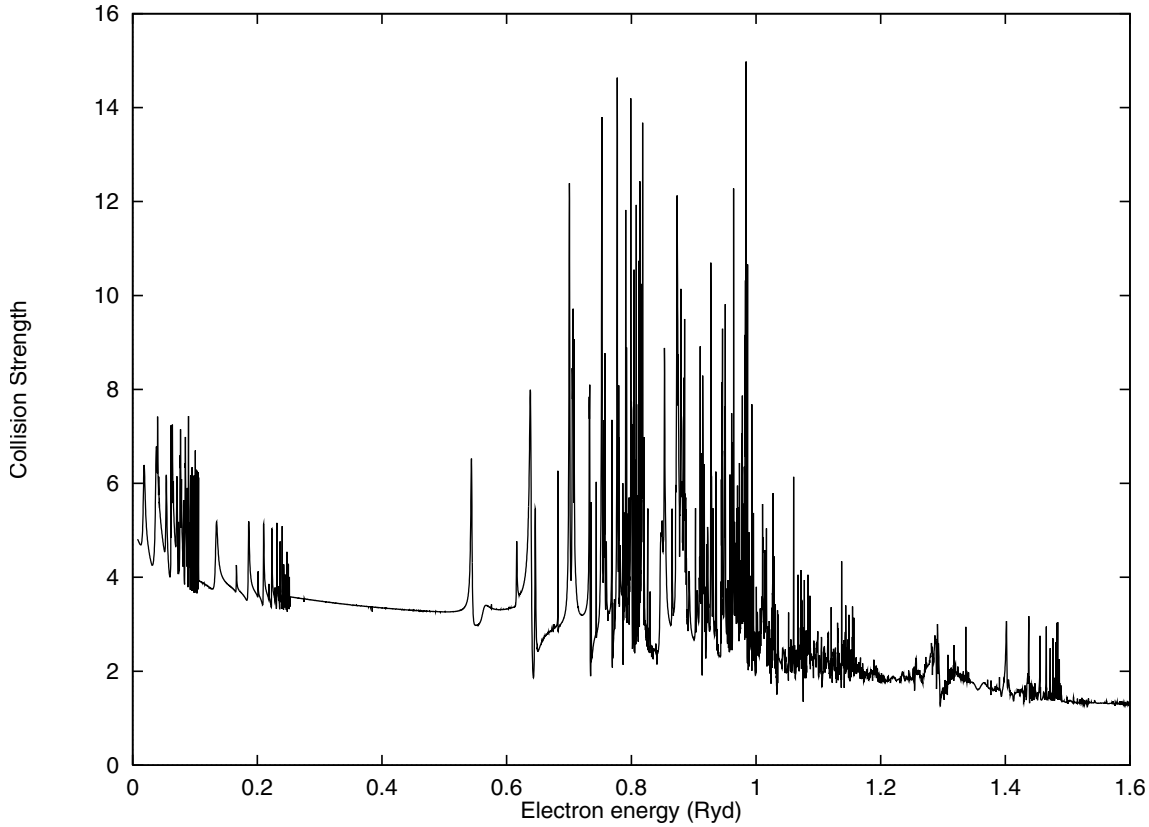

Fig. 1. Collision strength for the forbidden $3s^2 3p^4\ {}^3P_1$–$3s^2 3p^4\ {}^3P_2$ transition in Cl II as a function of electron energy (Ryd) in the thresholds energy region.

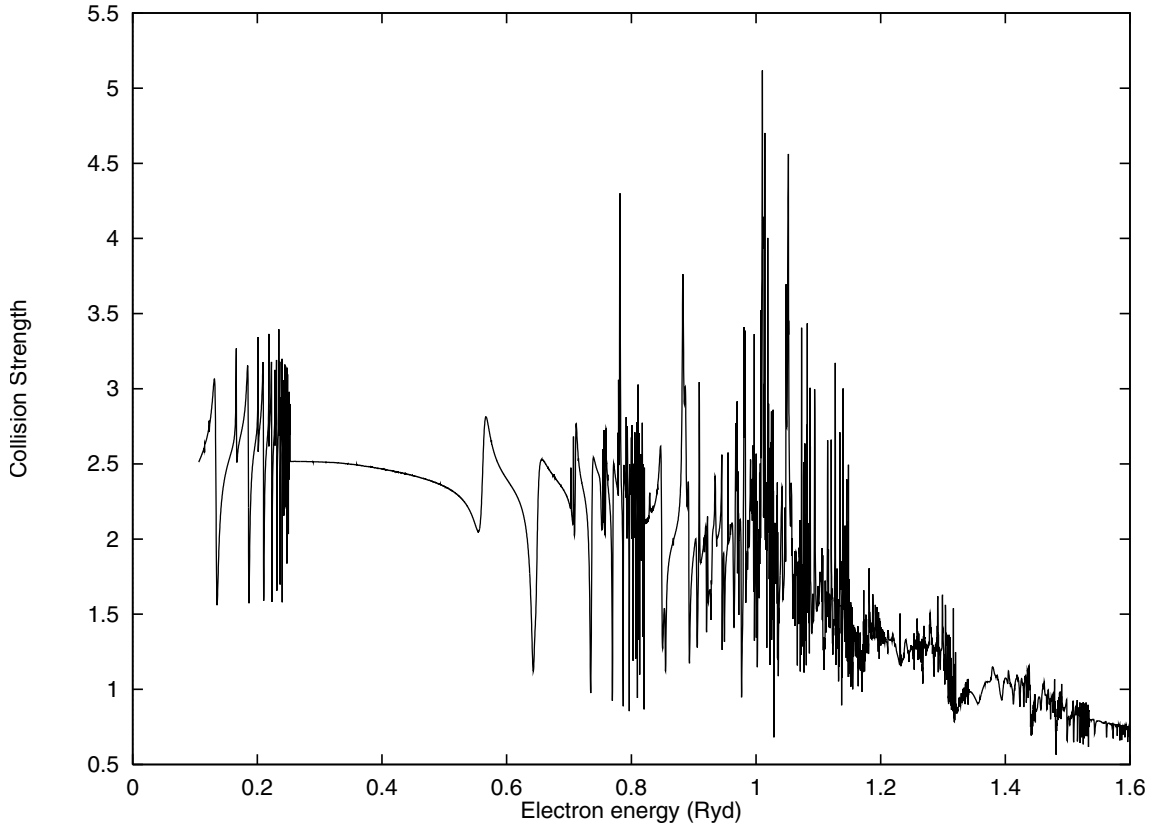

Fig. 2. Collision strength for the forbidden $3s^2 3p^4\ {}^3P_1$–$3s^2 3p^4\ {}^1D_2$ transition in Cl II as a function of electron energy (Ryd) in the thresholds energy region.

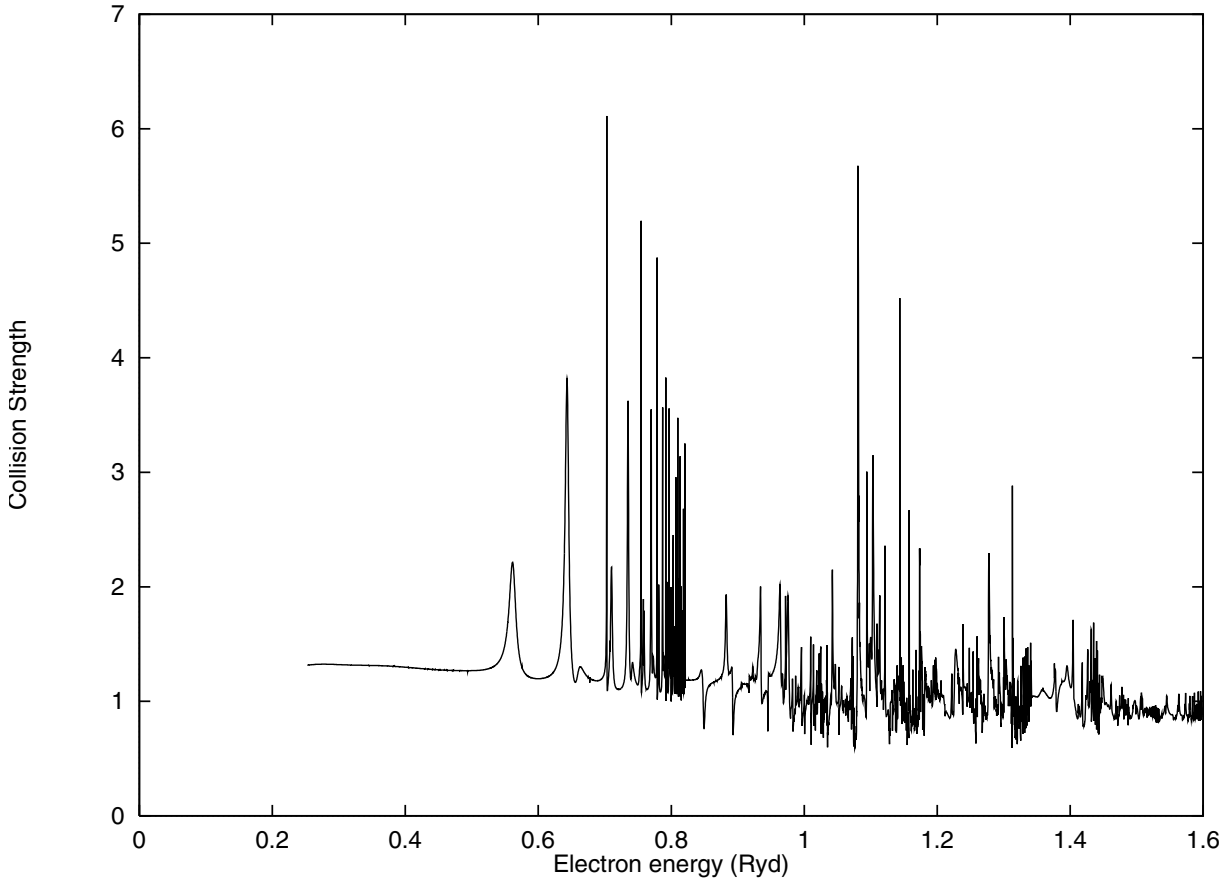

Fig. 3. Collision strength for the forbidden $3s^23p^4\ ^1D_2$–$3s^23p^4\ ^1S_0$ transition in Cl II as a function of electron energy (Ryd) in the thresholds energy region.

the $3s^23p^4\ ^1D_2$–$3s^23p^4\ ^1S_0$ transition shown in Fig. 3 of the present paper and Fig. 10 of their paper. The differences in background collision strengths are perhaps caused by the differences in the wavefunctions used in the two calculations.

We have plotted collision strengths as a function of electron energy in the above highest excitation threshold region from 1.6 Ryd to 16.6 Ryd in Fig. 4 for the allowed $3s^23p^4\ ^1D_2$–$3s^23p^3(^2D^\circ)4s\ ^1D^\circ_2$ (solid curve), $3s^23p^4\ ^3P_1$–$3s^23p^3(^4S^\circ)4s\ ^3S^\circ_1$ (long-dashed curve) and $3s^23p^4\ ^1D_2$–$3s^23p^3(^2D^\circ)3d\ ^1P^\circ_1$ (short-dashed curve) transitions. The collision strengths in this energy region show smooth variation with energy. The collision strengths for allowed transitions show increasing trend with energy in the high energy region and depend on the oscillator strength of the transitions (Eq. (3)). It is clear from Fig. 4 that the $3s^23p^4\ ^1D_2$–$3s^23p^3(^2D^\circ)4s\ ^1D^\circ_2$ transition is the strongest of the three allowed transitions.

The effective collision strengths are calculated by taking into account important resonance effects. These are obtained by integrating resonant collision strengths below the highest excitation threshold and smooth collision strengths above the highest threshold over a Maxwellian distribution of electron energies (Eq. (7)). In Table 2 we present effective collision strengths for all transitions between the $3s^23p^4\ ^3P_{0,1,2}$, $^1D_2$ and $^1S_0$ levels and from these levels to the 38 fine-structure levels of the excited configurations at electron temperatures from $\log T = 3.3$ to 6.0 K. The experimental wavelengths of

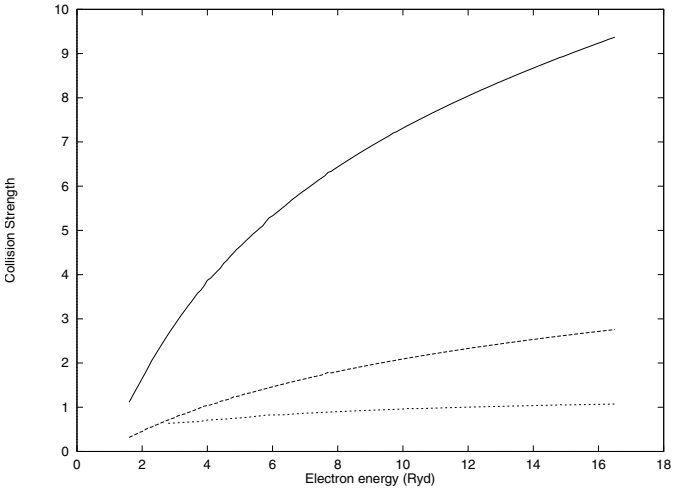

Fig. 4. Collision strength for the allowed $3s^23p^4\ ^1D_2$–$3s^23p^3(^2D^\circ)4s\ ^1D^\circ_2$ (solid curve), $3s^23p^4\ ^3P_1$–$3s^23p^3(^4S^\circ)4s\ ^3S^\circ_1$ (long-dashed curve) and $3s^23p^4\ ^1D_2$–$3s^23p^3(^2D^\circ)3d\ ^1P^\circ_1$ (short-dashed curve) transitions in Cl II as a function of electron energy (Ryd) above the highest excitation threshold.

transitions are also listed in Table 2. For many transitions the resonance effects in collision strengths enhance the effective collision strengths substantially in the lower temperature region. It may be noted that we presented effective collision

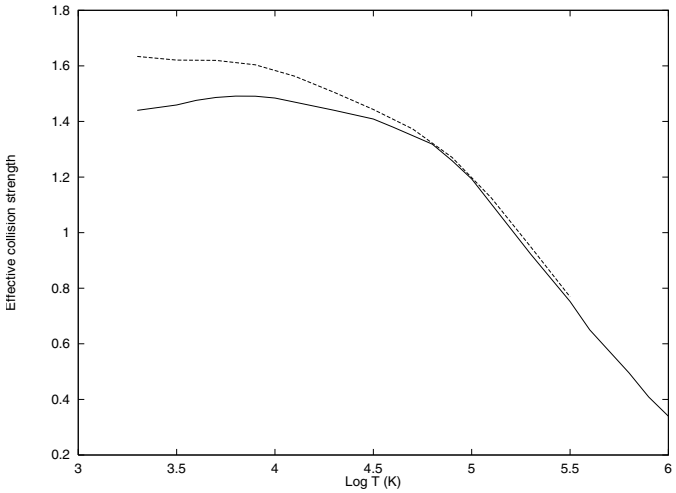

Fig. 5. Effective collision strength for the forbidden $3s^23p^4\ ^3P_0$–$3s^23p^4\ ^3P_1$ transition in Cl II as a function of log T (K). Solid curve, present results; dashed-curve, Wilson & Bell.

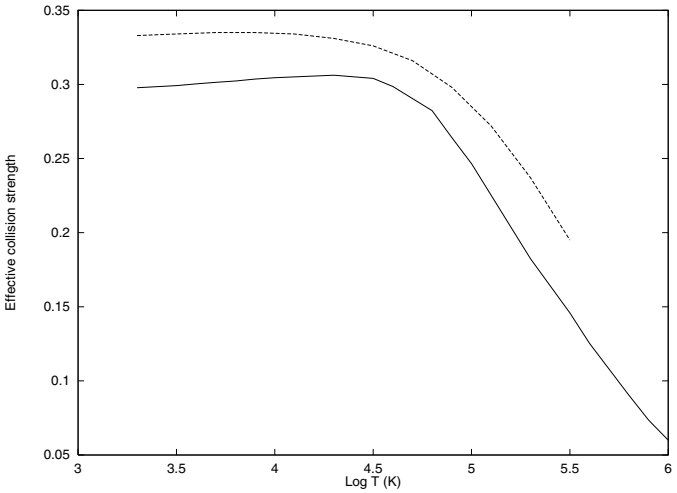

Fig. 7. Effective collision strength for the forbidden $3s^23p^4\ ^3P_1$–$3s^23p^4\ ^1S_0$ transition in Cl II as a function of log T (K). Solid curve, present results; dashed-curve, Wilson & Bell.

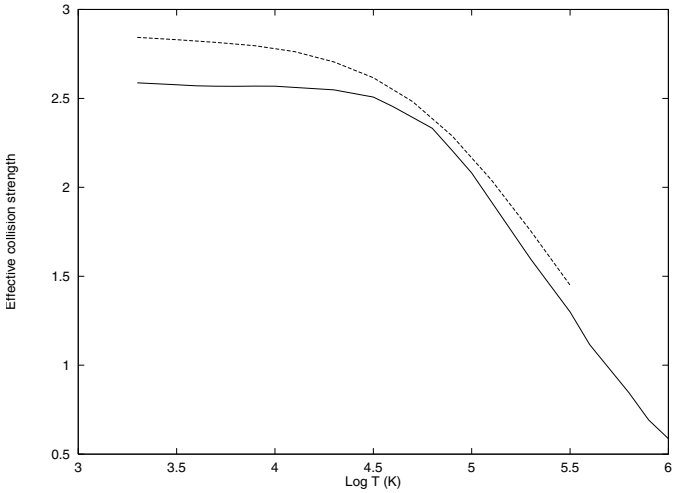

Fig. 6. Effective collision strength for the forbidden $3s^23p^4\ ^3P_1$–$3s^23p^4\ ^1D_2$ transition in Cl II as a function of log T (K). Solid curve, present results; dashed-curve, Wilson & Bell.

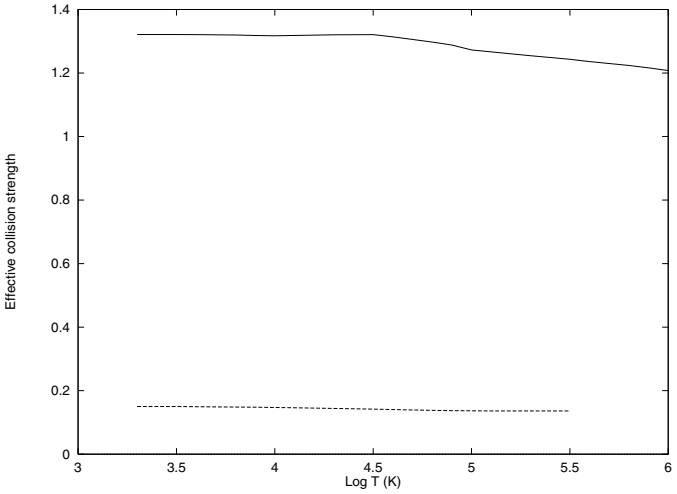

Fig. 8. Effective collision strength for the forbidden $3s^23p^4\ ^1D_2$–$3s^23p^4\ ^1S_0$ transition in Cl II as a function of log T (K). Solid curve, present results; dashed-curve, Wilson & Bell.

strengths for 43 fine-structure levels because the results for higher excitation levels (44−51) may not be accurate. The transitions involving these higher excitation levels are less accurate because of the neglect of coupling to levels that lie below and above. The main purpose of these levels in our calculation is to account for their strong coupling with lower levels.

Wilson & Bell (2002) presented effective collision strengths for 10 fine-structure transitions among the ground $3s^23p^4$ configuration levels that can be compared with our results. Their results are normally larger than the present results, particularly at lower temperatures. Our results for the forbidden $3s^23p^4\ ^3P_0$–$3s^23p^4\ ^3P_1$, $3s^23p^4\ ^3P_1$–$3s^23p^4\ ^1D_2$, $3s^23p^4\ ^3P_1$–$3s^23p^4\ ^1S_0$ and $3s^23p^4\ ^1D_2$–$3s^23p^4\ ^1S_0$ transitions are compared with their results in Figs. 5–8 respectively. Our results are shown by solid curve, while the results of Wilson & Bell (2002) are shown by the dashed curve. Our results are lower than Wilson & Bell (2002) at log $T \leq 5.0$ for the $3s^23p^4\ ^3P_0$–$3s^23p^4$–$^3P_1$ and $3s^23p^4\ ^3P_1$–$3s^23p^4\ ^1D_2$ transitions by upto 12%. The effective collision strengths from our calculation for the $3s^23p^4\ ^3P_1$–$3s^23p^4\ ^1S_0$ transition (Fig. 7) are lower at all temperatures than the values of Wilson & Bell (2002). The discrepancies are mostly caused by the difference in background collision strengths away from resonances. There are large discrepancies for the forbidden $3s^23p^4\ ^1D_2$–$3s^23p^4\ ^1S_0$ transition between the two calculations as shown in Fig. 8. Wilson & Bell (2002) appear to have made an error in computing effective collision strengths for this transition because the differences in collision strengths from the two calculations do not account for the large difference.

4. Summary

We have presented elaborate calculations of collision strengths and effective collision strengths for transitions between the $3s^23p^4\ ^3P_{0,1,2}$, $^1D_2$ and $^1S_0$ levels and from these levels to 38 excited levels of Cl II. Our results are presented over a wide

electron temperature range suitable for use in astrophysical plasma modeling. In our work we used non-orthogonal orbitals both for the representation of target wavefunctions and for the representation of scattering functions. The use of non-orthogonal orbitals considerably simplifies the structure of the bound part of the close-coupling expansion, that leads to substantial reduction in pseudo-resonances. We used ICFT method to transform LS-coupled K-matrices to K-matrices in intermediate coupling. This method should lead to improved accuracy compared to standard transformation method used by Wilson & Bell (2002) to calculate level-to-level electron impact excitation collision strengths. Our calculation should also be accurate because of the inclusion of additional 11 excited states in the close-coupling expansion to ensure convergence of results for fine-structure transitions presented in our work. Significant differences with earlier calculation (Wilson & Bell 2002) are noted for some transitions which may have important consequences for astrophysical plasma diagnostics.

Acknowledgements. This research work was supported by NASA grant NAG5-13340 from the Planetary Atmospheres Program.

References

Berrington, K. A., Eissner, W. B., & Norrington, P. H. 1995, Comput. Phys. Commun., 92, 290
Berrington, K. A., & Nakazaki, S. 2002, At. Data Nucl. Data Tables, 82, 1
Burgess, A., Hummer, D. G., & Tully, J. A. 1970, Phil. Trans. R. Soc. A, 266, 225
Burke, V. M., & Noble, C. J. 1995, Comput. Phys. Commun., 85, 471
Feldman, P. D., Thomas, B. A., Berman, A. F., et al. 2001, ApJ, 554, L123
Froese Fischer, C. 1991, Comput. Phys. Commun., 64, 369
Griffin, D. C., Badnell, N. R., & Pindzola, M. S. 1998, J. Phys. B, 31, 3713
Hibbert, A. 1975, Comput. Phys. Commun., 9, 141
Krueger, T. K., & Czyzal, S. J. 1970, Proc. R. Soc. Lond. A, 318, 531
Küppers, M. E., & Schneider, N. M. 2000, Geophys. Res. Lett., 27, 513
Tayal, S. S. 2003, J. Phys. B, 36, 3239
Wilson, N. J., & Bell, K. L. 2002, MNRAS, 331, 389
Zatsarinny, O., & Froese Fischer, C. 1999, Comput. Phys. Commun., 124, 247
Zatsarinny, O., & Tayal, S. S. 2001, J. Phys. B, 34, 3383